

Dynamic 3D Modelling of the Human Left Ventricle

K.K.O.S. Gunarathne¹, R.G.N. Meegama¹ and J. Herath²

¹*Department of Computer Science, Faculty of Applied Sciences, University of Sri Jayewardenepura
Gangodawila, Nugegoda, Sri Lanka*

rgn@sci.sjp.ac.lk

²*Sri Jayewardenepura General Hospital, Nugegoda, Sri Lanka*

Abstract—Visualization and quantification of cardiac function is important in diagnosing and management of heart diseases. As quantitative analysis performed on the images is crucial to understand the heart mechanics, an accurate diagnosis of heart conditions can be done if clear visualization of ventricular volume, mass and function are obtained from echo-cardiograph images. This paper presents a technique to develop a dynamic three dimensional model of the left ventricle of the human heart to illustrate both the shape and motion of the ventricle along a cardiac cycle. The proposed methodology includes a multistage approach that involves a pipeline of image processing routines such as filtering, contrast stretching and binary morphology to isolate heart tissues. Subsequently, cubic spline curves are used to generate a smooth surface of the heart muscle using a set of control points extracted from the locations of boundaries of the heart muscle. A complete pulse included 40 images and it takes an average of 16.0665 seconds for the model to deform over a pulse.

Keywords— left ventricle, echocardiography, dynamic modelling

I. INTRODUCTION

Visualization and quantification of cardiac function is important in diagnosing and managing heart diseases. In recent times, heart failure has caused high morbidity and mortality rates in humans with the incidence and prevalence are increasing due to the use of alcohol, physical inactivity, an unhealthy diet [9].

With current diagnosing techniques such as echocardiography, cardiac MRI and CT, it is possible to obtain clear grey scale images in 2D with patient data [10]. These images can be used to extract cardiac information of the patient using computer assisted tools. Noninvasive techniques are much popular and acceptable for the study of the human heart *in vivo*. Present noninvasive diagnosing techniques, as mentioned earlier, provide only a 2D view of the organ taken at a particular instance of time. Some of these images are quite confounded by external factors making it difficult to visualize the actual anatomy of the heart. Hence, it requires analyzing a series of images taken at different views at different times to arrive at clinically accurate conclusions. Such an analysis is a manual process that consumes time and requires expertise knowledge. Moreover, these images can provide only a qualitative analysis at the hands of a medical practitioner.

A quantitative analysis performed on the images is crucial to understand the mechanics of the heart. This gives us a framework to investigate the shape and motion of the heart throughout a cardiac cycle by giving important parameters of study like strain and strain rate of myocardium.

Pathological investigations of heart diseases are mainly concerned on the left ventricle (LV) of the heart because the consequence of a heart disease is better visualized by the left ventricle. Left ventricular hypertrophy is one such instance where the myocardium of the left ventricle gradually becomes thick and loses its ability to relax due to a cardiovascular disease [11].

Biomechanics is the field of study that analyses mechanical properties of biological systems and how the structure of a system deforms when subjected to certain forces. These models are now becoming popular in clinical practice as a tool in surgical planning because of their ability to display deformations on soft tissues in real time. Such therapeutic simulations can be tried out with the model before the actual surgery [1].

The main objective of the work presented in this paper is to digitally reconstruct the shape and motion of the left ventricle of the heart by a three dimensional deformable model using a series of image processing routines.

II. RECENT WORK

Santos et. al. [2] have used spatial linear space domain filter with a 3x3 neighborhood to remove noise from echo-cardiograph images and then a histogram modification is used to enhance endocardial and epicardial boundaries of the left ventricle. The histogram modification is manipulated by background subtraction and linear contrast stretching. Median filter is also discussed as an effective noise filtering technique for echo-cardiographs.

A morphological filtering technique to remove noise in the ventricle cavity in echocardiograph images is presented in [3]. Although the method performs well in removing noise in the cavity, the resulting image exhibits discontinuities at the edges.

In [4] and [5], multistage hybrid segmentation methods which combine morphological reconstruction and fast marching algorithms are proposed to segment dynamic CT images of the beating heart. Quantitative evaluation on 50

canine CT images against ground truth had demonstrated a similarity index of 0.956.

A multimodality segmentation algorithm to segment the LV from cardiac images based on deformable models is presented in [6]. Four parameters govern forces on the model and satisfy an Euler-Lagrange equation at the equilibrium. Further, it gives a methodology to incorporate temporal information to the edge detection to filter out spurious edges.

III. PROPOSED METHODOLOGY

The proposed methodology includes a multistage approach where a series of raw echo images is taken and cropped into a fixed size such that they all significantly represent the LV region of interest (ROI). Then, the fiducial marks present in these images are removed as they might affect post processing tasks. Median filtering [7] is applied to reduce speckle noise (Fig. 1(b) and 1(e)) and subsequently, a linear contrast stretch is applied to enhance a selected intensity range highlighting the difference between the myocardium and the blood pool (Fig. 1(e) and 1(f)).

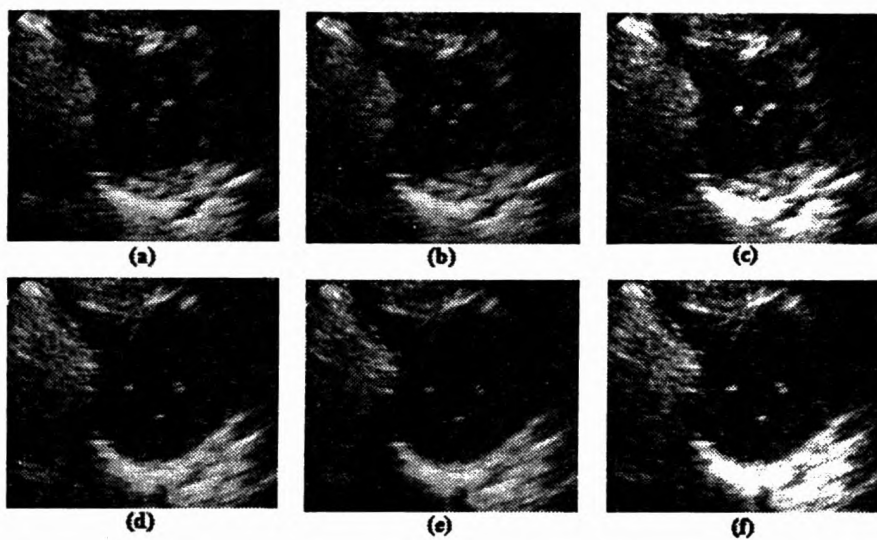


Figure 1: Pre-processing step (short axis-base): (a) & (d) Original images, (b) & (e) median filtering, (c) & (f) contrast stretching.

The above pre-processed images are taken as the input to the segmentation process which is also a multistage procedure as seen in Fig. 2. First, binary images are obtained by a global thresholding scheme applied for all the short axis images whereas an adaptive thresholding (window size 130 and threshold 0.01) is applied for long axis images. The resulting image is then recursively eroded using a disk shaped structuring element until the LV cavity is completely separated from its connected regions. It is followed by labelling the connected components to label maximally connected regions of foreground pixels in the resulted binary image. Then, using *a priori* knowledge, the LV is extracted by considering the average size of a human LV. The extracted LV is then recursively dilated with the same structuring element to recover lost pixels during the previous erosion. It is possible that some speckle noise may have been left out during the pre-processing stage. As such, morphological filling is applied at the next stage.

The segmented image is taken as the input to the boundary point extraction process. As the first step, the boundary of the LV is extracted by applying the Sobel filter. Then, a radial search is performed by rotating the image around its central axis and taking the boundary point at each 10° degree. The segmented image series obtained at $t = t_0$ is used to reconstruct the initial LV geometry in the 3D space. The model is defined in spheroidal coordinate system (λ, μ, θ) and the proposed steps are as follows:

First, the following are calculated in order to simplify the task.

- Centroid coordinates of the LV in every short-axis image slice: (x_c, y_c)
- Location of the base in a long-axis image slice: (x_b, y_b)
- Location of the apex in a long-axis image slice: (x_a, y_a)

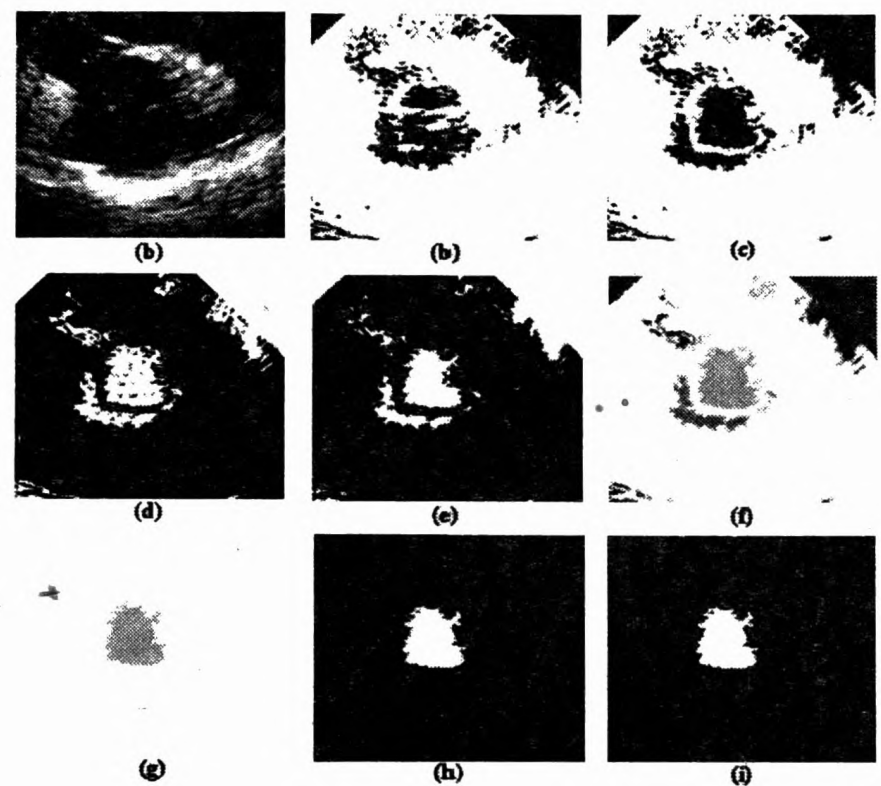


Figure 2: Output images of segmentation steps (short axis-apex): (a) pre-processing, (b) global thresholding, (c) boundary correction, (d) inverse binary image, (e) erosion, (f) connected component labelling, (g) extracted LV, (h) dilation and (i) morphological filling.

At first, the long axis image slices are used to obtain the distance from the apex to the base. This distance is used as an overall scale factor for a voxel. Subsequently, the segmented short-axis slices are transformed into 3D space using the transformation equation.

$$v_1 = T_c R T_d v_0$$

where $v_0 = (x_0, y_0, z_0)^T$ represent the homogeneous coordinates of a point in the 3D plane and $v_1 = (x_1, y_1, z_1)^T$ represents its transformed coordinate position as a 3D voxel. T_c , T_d and R represent translation and rotation matrices, respectively.

The images are placed in the 3D space by first translating them into the origin of the xyz coordinate system and rotated according to the angle in which they are acquired by the probe. Subsequently, the images are again translated

along the z axis such that the base short axis plane is located at distance d from the origin, mid ventricular plane at $2d/3$ distance and apex plane located at $d/5$ distance as in Fig. 3.

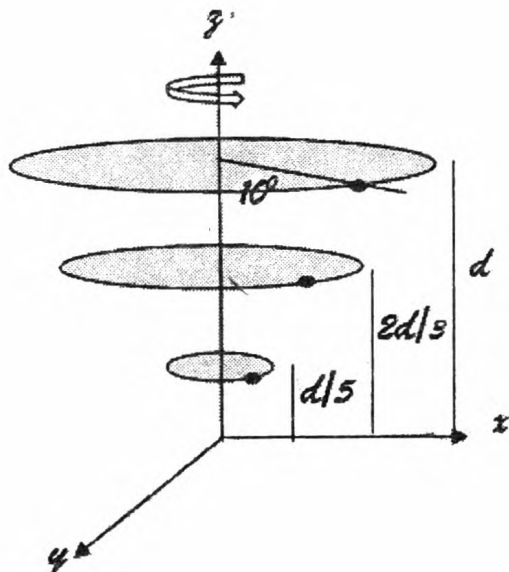


Figure 3. Extraction of control points from a filtered image by rotating an axis about the centroid.

Although the segmented slices are placed at its correct position in the voxel, a continuous volume cannot be obtained until discrete locations of control points are known. Hence, the volume is re-sampled and reconstructed in 3D by a finite number of points sufficient to represent the LV shape. A straight line is rotated around the z axis and at every 10^{th} degree and a control point is taken at the intersecting point with the short-axis image.

Reconstruction of the initial geometry is done using cubic spline curves with Lagrange end conditions. After constructing the wireframe, Gouraud lighting model is applied to obtain a smooth shading.

Considering that every image plane is spatially fixed during a heart beat, some of the structures move in or out from the plane. However, such through-plane motion cannot be captured from data points on the image plane.

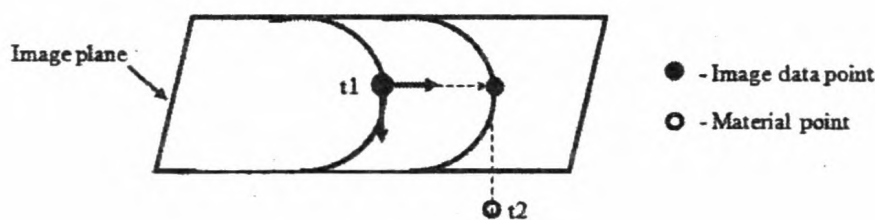


Figure 4. Image plane and material points.

Figure 4 shows the location of image data points at two different time intervals t_1 and t_2 . Initially, at t_1 , the image data point coincides with the material point. However, the motion of the image data point between these two time intervals approximates to the components on the image plane.

However, the motion of the material point can be captured from images at two perpendicular directions taken at t_2 . From the slice of a short axis image, we can extract the x, y

components which contain the in-plane motion. Further, from the long axis image, we can extract the z-component containing the through-plane motion.

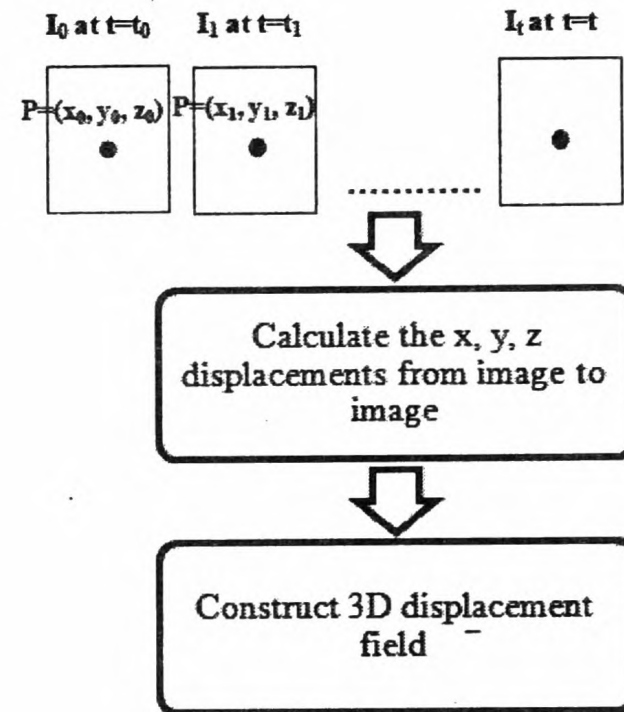


Figure 5. Stages in calculating the 3D displacement field.

Let (x_0, y_0, z_0) and (x_1, y_1, z_1) be two coordinate positions of a single material point in two consecutive frames. First, the x, y, z displacements are calculated, respectively, by:

$$d_x = x_1 - x_0 \quad d_y = y_1 - y_0 \quad d_z = z_1 - z_0$$

Then, a displacement vector v is constructed as

$$v = (d_x, d_y, d_z)$$

Likewise, by calculating and integrating v for all the boundary points in all the planes, we can obtain the 3D displacement field. Extraction of the height of LV is shown in Fig. 6.

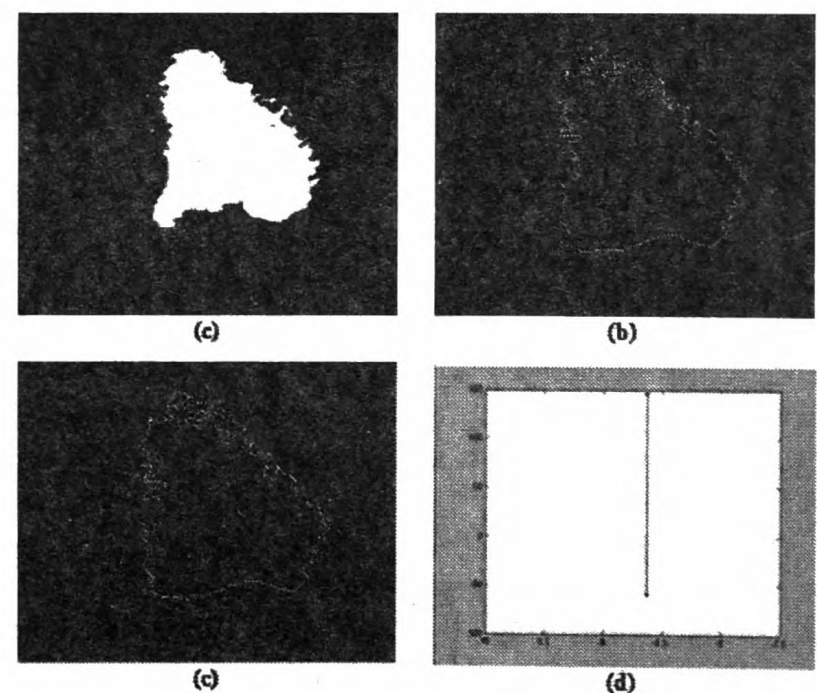


Figure 6: Outputs of LV height extraction from long axis images. (a) segmented long axis LV, (b) boundary extracted, (c) maximum and minimum points and (d) estimated height.

Before constructing a method to deform the initial geometry the continuous material domain (u, v) is tessellated into a mesh of M elements. We approximate x as the weighted sum of piecewise polynomial functions N^i such that

$$x(u, v, t) = \sum_{i=0}^n N^i(u, v)q^i(t)$$

where q^i is a vector of the nodal variables associated with the mesh node i . The model is deformed according to the following equation

$$q^{t+1} = q^t + TD^{x,y,z,t}$$

where T is a transformation matrix concerning translation and D the displacement field calculated

IV. RESULTS AND DISCUSSION

Pre-processing

Typically, every echo-cardiograph image has the presence of speckle noise [8]. If not removed, the speckle noise will severely obstruct the identification of object boundaries in the image. Therefore, it is very important to remove such speckle noise from the images as much as possible in the pre-processing stage. The structure of a human heart is complex with images having much delicate details such as the mitral valve and papillary muscle. It is noticed that although much of the speckle noise can be removed after applying the Gaussian filter, miniature details are not preserved. On the other hand, the median filter is capable of preserving these fine details and also reducing noise in considerable amount from the images.

Extraction of left ventricle

The proposed segmentation method used thresholding in two different ways. For the long axis window, an adaptive thresholding produced better results than a global threshold. The main value of a window is selected as the optimal threshold. However, as this method does not produce better results for short axis images, a global threshold is applied to extract the inner cavity from the pre-processed images.

While morphological operations resulted in a finer left ventricle output, morphological filling is helpful in obtaining a continuous image where speckle noise in ultrasound often leads to discontinuities in the segmented slice. Further, this results in segmented image slices to have rough edges.

One of the difficulties came across in research is manual corrections during extraction of the LV boundary which requires time and medical expertise to identify the endocardium and epicardium.

Figure 7 shows the variations of the average radiance of the short axis images over time. As seen, it starts from end-

diastole having the maximum average radiance and then gradually decreases as the systolic phase starts. Then, at $t = 22$, at the end-systole, it has the minimum average radiance.

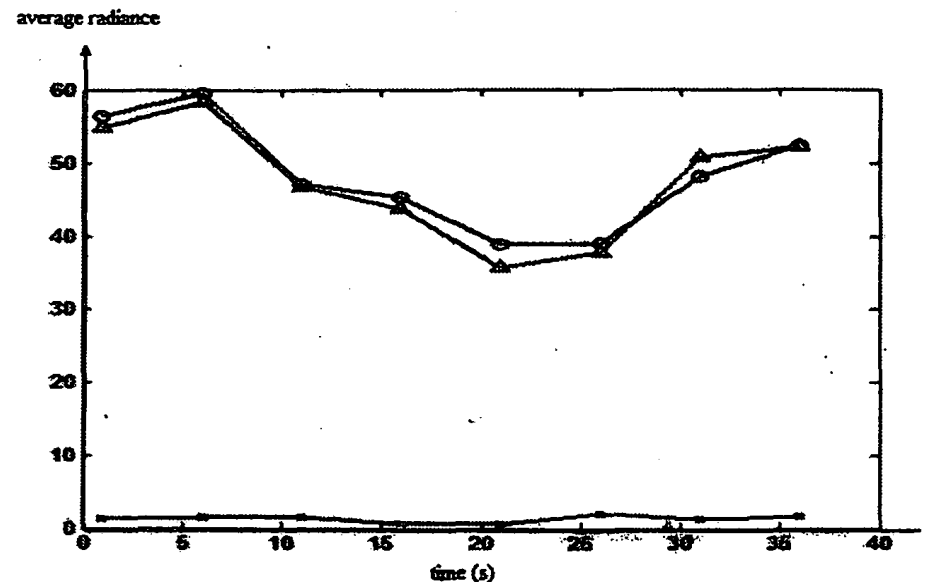


Figure 7. Average radiance of short axis images with respect to time.

The construction of the initial geometry of the LV involves recreation of the ventricle shape for the end-diastolic. The information about the shape is taken from the image data related to the end diastolic as well as from prior expertise knowledge. Splines are used to reconstruct the ventricle surface due inherent smoothness properties. The shape of the LV is acquired using 108 control points. Compared to finite element geometry, usage of splines has two advantages: smoothness and continuity. Such smoothness and continuity criteria are not prevalent in finite element modelling with Delaunay triangulation. Different orientations of the initial geometry of the LV are given in Fig 8. Also, as shown in Fig. 9, the LV has deformed to the end-systole having the smallest volume.

A complete pulse included 40 images and it takes an average of 16.0665 seconds for the model to deform over a pulse. The average is calculated for 10 complete pulses. The images are taken from a healthy male subject with a pulse rate of 78 bpm, taking 0.7692 seconds to complete a pulse in real time. The model shows a 15.2937 seconds delay compared to an actual scenario.

V. CONCLUSION

Patient specific biomechanical models would be the most promising tool for diagnosing heart diseases. Unlike any image modality used in clinical practice, these models are capable of illustrating every small detail of the shape and motion of the ventricles. However, the complex structure of the heart has made it difficult to archive such a 4D deformable model.

Constructing a deformable model using echo-cardiograph images is a challenging task as in a majority of cases, the images are so hampered by speckle noise to an extent that the fine details cannot be fully recovered using existing techniques. Unlike ultrasound, MRI offers a technique called tagging which allows us to estimate the

motion of material points of the heart muscle in a more accurate manner [12]. For classification, a statistical method such as Bayesian techniques would produce a better results than thresholding.

All the experiments are carried out using images of healthy volunteers. It is prudent to test the performance of the proposed technique on images belonging to patients with heart diseases before it can be used in a clinical setup.

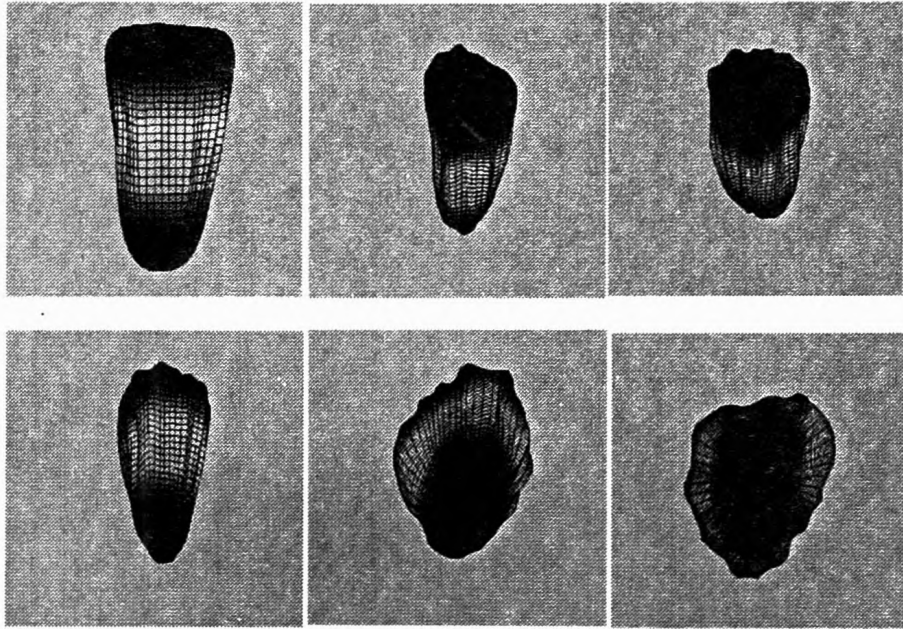


Figure 8: Different orientations of the initial geometry of

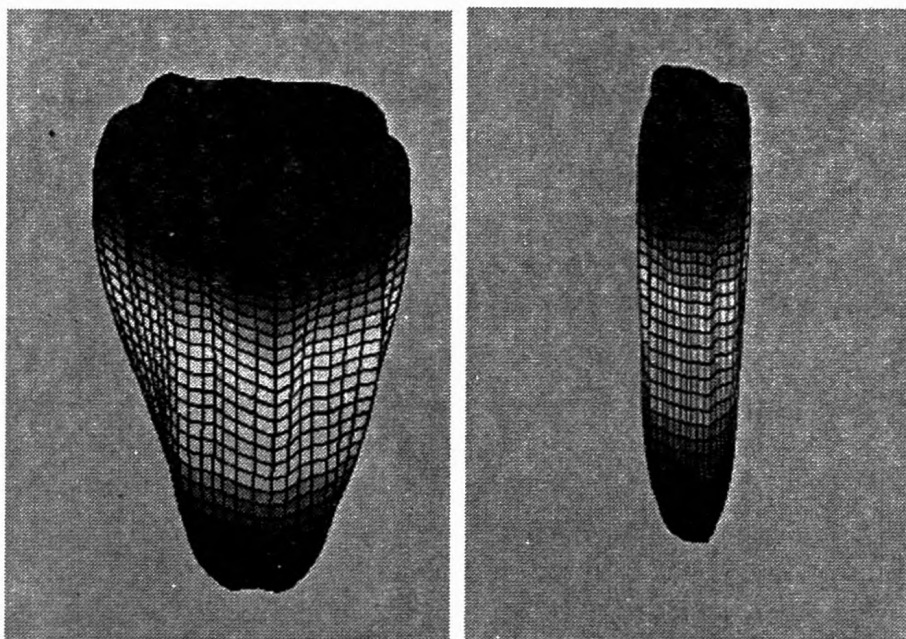


Figure 9: (left) end-diastolic and (right) end-systolic of the dynamic left ventricle.

REFERENCES

- [1] Koerkamp, M. A. M., Snoep, G., Muijtjens, A. M. M., & Kemerink, G. J. (1999). Improving contrast and tracking of tags in cardiac magnetic resonance images. *Magnetic Resonance in Medicine*, 41(5), 973-982.
- [2] Hammoude, A. (1998). Endocardial border identification in two-dimensional echocardiographic images: review of methods. *Computerized Medical Imaging and Graphics*, 22(3), 181-193.
- [3] Choy, M. M., & Jin, J. S. (1996, April). Morphological image analysis of left-ventricular endocardial borders in 2D echocardiograms. In *Medical Imaging 1996* (pp. 852-863). International Society for Optics and Photonics.
- [4] Gu, L. (2004). Dynamic Heart Modeling Based on a Hybrid 3D Segmentation Approach. In *Medical Imaging and Augmented Reality* (pp. 237-244). Springer Berlin Heidelberg.
- [5] Montillo, A., Metaxas, D., & Axel, L. (2002). Automated segmentation of the left and right ventricles in 4D cardiac SPAMM images. In *Medical Image Computing and Computer-Assisted Intervention—MICCAI 2002* (pp. 620-633). Springer Berlin Heidelberg.
- [6] Carlsson, M., Ubachs, J. F., Hedström, E., Heiberg, E., Jovinge, S., & Arheden, H. (2009). Myocardium at risk after acute infarction in humans on cardiac magnetic resonance: quantitative assessment during follow-up and validation with single-photon emission computed tomography. *JACC: Cardiovascular Imaging*, 2(5), 569-576.
- [7] Eng, H. L., & Ma, K. K. (2001). Noise adaptive soft-switching median filter. *Image Processing, IEEE Transactions on*, 10(2), 242-251.
- [8] Zheng, Y., Barbu, A., Georgescu, B., Scheuring, M., & Comaniciu, D. (2008). Four-chamber heart modeling and automatic segmentation for 3-D cardiac CT volumes using marginal space learning and steerable features. *Medical Imaging, IEEE Transactions on*, 27(11), 1668-1681.
- [9] Denney Jr, Thomas S. "Identification of myocardial tags in tagged MR images without prior knowledge of myocardial contours." *Information Processing in Medical Imaging*. Springer Berlin Heidelberg, 1997.
- [10] Petersen, S. E., Selvanayagam, J. B., Wiesmann, F., Robson, M. D., Francis, J. M., Anderson, R. H., Watkins, H., and Neubauer, S. (2005). Left ventricular non-compaction insights from cardiovascular magnetic resonance imaging. *Journal of the American College of Cardiology*, 46(1), 101-105.
- [11] Schiller, N. B., Shah, P. M., Crawford, M., DeMaria, A., Devereux, R., Feigenbaum, H., Gutgesell, H., and Schnittger, I. (1988). Recommendations for quantitation of the left ventricle by two-dimensional echocardiography. American Society of Echocardiography Committee on Standards, Subcommittee on Quantitation of Two-Dimensional Echocardiograms. *Journal of the American Society of Echocardiography: official publication of the American Society of Echocardiography*, 2(5), 358-367.
- [12] Denney Jr, T. S. (1997, January). Identification of myocardial tags in tagged MR images without prior knowledge of myocardial contours. In *Information Processing in Medical Imaging* (pp. 327-340). Springer Berlin Heidelberg.